ECS Advances

Experimental Benchmarking for High-Reproducibility, Cross-Institutional Evaluation of Iron Redox Electrochemistry

To cite this article before publication: Benjamin Ketter *et al* 2026 *ECS Adv.* in press https://doi.org/10.1149/2754-2734/ae6089

Experimental Benchmarking for High-Reproducibility, Cross-Institutional Evaluation of Iron Redox Electrochemistry

Journal:	*ECS Advances*
Manuscript ID	ECSA-100359.R2
Manuscript Type:	Research Paper
Date Submitted by the Author:	15-Apr-2026
Complete List of Authors:	Ketter, Benjamin; Argonne National Laboratory, Materials Science Division; The University of Chicago, Pritzker School of Molecular Engineering LUO, JIANG; Argonne National Laboratory, Sun, Yunkai; Argonne National Laboratory, Chemical Sciences and Engineering Division Lvovich, William; Case Western Reserve University, Department of Chemical Engineering Sinclair, Nicholas; Case Western Reserve University, Chemical Engineering Yang, Zhenzhen; Argonne National Laboratory, Chemical Sciences and Engineering Connell, Justin; Argonne National Laboratory, Materials Science Division
Keywords:	Electrodeposition, Electrowinning, Electroanalytical Electrochemistry

Experimental Benchmarking for High-Reproducibility, Cross-Institutional Evaluation of Iron Redox Electrochemistry

Benjamin Ketter,[1,2,3] Jiang Luo,[1,2] Yunkai Sun,[1,4] William Lvovich,[1,5,*] Nicholas Sinclair,[1,5] Zhenzhen Yang,[1,4] and Justin G. Connell[1,2,3,z]

[1]Center for Steel Electrification by Electrosynthesis (C-STEEL), Argonne National Laboratory, Lemont, Illinois 60439, USA
[2]Materials Science Division, Argonne National Laboratory, Lemont, Illinois 60439, USA
[3]Pritzker School of Molecular Engineering, University of Chicago, Chicago, Illinois 60637, USA
[4]Chemical Sciences and Engineering Division, Argonne National Laboratory, Lemont, Illinois 60439, USA
[5]Department of Chemical and Biomolecular Engineering, Case Western Reserve University, Cleveland, Ohio 44106, USA

[*]Electrochemical Society Student Member.
[z]E-mail: jconnell@anl.gov

Abstract

We present a practical case study standardizing experimental protocols between collaborators with the goal of understanding ferrous iron (Fe^{2+}) chemistry and improving the iron deposition reaction for energy-efficient, electrochemical iron production. The study of iron reactions can be difficult, as aqueous iron electrolytes exhibit complex behaviors that can lead to differing interpretation of ostensibly similar experiments. The question we want to answer: *are we studying the same chemistry?* Our protocols address inherent challenges such as the tendency for Fe^{2+} to spontaneously oxidize to ferric iron (Fe^{3+}) and the production of hydrogen at the potentials of interest. Our standardized protocol, executed by four collaborators in different labs and institutions, yields high-reproducibility results, and identified glassy carbon electrode surface quality and Fe^{3+} impurities in the salt as key factors with outsized effects on cyclic voltammetry measurements. The process of developing the protocols helped to troubleshoot underlying issues that created poorer reversibility and reproducibility. This study highlights the fact that even nominally straightforward electrochemical systems can yield vastly different outcomes due to

small differences in experimental preparation and serves as a useful example for creating transparent and achievable standards for the generation of reliable datasets that can be widely used and shared.

Introduction

The production of 1.9 billion tons of steel per year accounts for 7% of global energy consumption, which is a reflection steel's ubiquity and critical role in the construction of buildings and equipment.[1] The chief technology used to manufacture iron from raw materials involves reducing the iron ore using coke as a reductant in a high-temperature environment (1600 °C).[2] Other than incremental improvements in efficiency and yield, the technology has remained essentially constant for over 600 years. Fundamentally new approaches, such as electrochemical methods, are required to enable this process to consume less energy while reducing iron from ore to a usable, purified metallic form. However, the study of iron reactions can be difficult, as aqueous iron electrolytes exhibit complex behaviors that can lead to differing interpretation of ostensibly similar experiments across the scientific community.

The fundamental electrochemical reduction of Fe^{2+} to Fe^0 happens as follows:

$$Fe^{2+} + 2e^- \rightarrow Fe^0 \quad (E° = -0.44 \text{ V vs. SHE}) \qquad \text{Equation 1}$$

Where V vs. SHE is the potential versus the standard hydrogen electrode (SHE). The aqueous system presents unique challenges, such as the tendency for Fe^{2+} to spontaneously oxidize to Fe^{3+}, iron metal's tendency to evolve H_2 at Fe^{2+} reduction potentials, and solubility limits at higher pH.[3] Compared to other fields in electrochemistry, such as batteries or solar cells, there is less precedent for studying iron reduction.[4] Previous work has been done in the context of engineering bath formulations for specialty electroplating applications or for developing iron redox flow batteries, which utilize the Fe^{2+} to Fe^0 reduction as a means of storing electricity.[3,5-14] Many prior studies concerning corrosion characterize the galvanic oxidation of Fe^0 to Fe^{2+} at open circuit voltage or low overpotentials; however, they omit many important aspects relevant to the reduction of iron, even in cyclic voltammetry (CV) studies that probe potentials below the plating potential of iron.[15-17] Our work studying the chemistry of high-overpotential reduction of iron explores new and unique aspects of the underlying chemistry; with it comes new and unexpected challenges to understanding and contextualizing differences observed.

There have been many efforts to standardize or create best practices in the field of electrochemistry as a whole; researchers have tried many different methods to extrapolate the reported results on some basis of ground truth and carry forward recommendations for how to improve research in the field.[18] The field of electrocatalysis has endeavored to standardize

experimental protocols and data reporting.[19,20] Such efforts are detailed and focus on best practices of quantifying a material's activity – how to clean the cell, what kind of water to use, what kind of reference electrode to use, or how to study the specific reactions of interest.[21,22] In other studies, multiple scientists screen a large array of materials such that general trends can be identified without the confusion of different institutions or scientists.[20] "Round robins" have also been conducted seeking to compare results between groups – a device with an identical design is tested between multiple labs or the same device itself is passed between labs.[23,24] The development and widespread commercialization of batteries, in particular lithium ion systems, has necessitated the standardization of protocols and reporting procedures as the technology has matured and enabled meta-analysis of performance metrics.[25-27] As efforts proceed to enable predictive analysis of lifetime and cell failure for enhanced safety and expedited materials qualification, reliable standardized protocols are gaining importance in the battery space as well.[28-31] In particular, the use of advanced artificial intelligence and machine learning algorithms necessitates a baseline element of comparability. The field of all-solid-state battery research has also acknowledged the challenge of reproducibility and standardization, with even small differences in the cell assembly and data reporting protocols creating a large impact on the observed performance.[32]

Establishing rigorous experimental benchmarks is critical for advancing electrochemical research, especially in the context of team- or center-based programs where multiple groups working on the same problem require a common language to contextualize their results against one another to collectively make progress. In all electrochemical systems, differences in the materials history, electrode surface quality, the presence of trace electrolyte impurities, cell cleanliness, and other incidentals of the measurement can produce different results that are extrinsic to the "true" properties and performance of a given system. The origins of these differences are lost once the results are distilled down to a single figure of merit that is quantitatively compared to its peers, leading to uncertainty throughout the literature about what truly constitutes an advance.[32-34] Our persisting question is: are we measuring the same chemistry? In the context of advancing the industrial-scale electrification of the iron smelting process, a baseline set of expectations helps us move beyond the routine challenges associated with electrochemical experiments toward learning new information about the fundamental chemistry of iron.

In this work we create a forward-looking set of standardized protocols and data collection methods to create a baseline standard of comparison between the data gathered by different groups in the Center for Steel Electrification by Electrosynthesis (C-STEEL). To ensure that results bear valuable comparisons in collaborations between institutions, we standardized our protocols and devised baseline studies to understand the underlying systematic and unavoidable errors inherent in salt impurities, instrumentation, electrode preparations, and experimental execution, to name several examples. The protocol development process, which utilized the aqueous electrolyte 0.1 M $FeSO_4$ as a baseline system, uncovered a surprisingly complex interplay between electrode and electrolyte chemistry that highlights the numerous inherent challenges associated with producing reliable and reproducible results, even for a nominally "simple" system. We identify glassy carbon (GC) electrode surface quality and Fe^{3+} impurities in the salt as key factors with outsized effects on the voltammetry. The process of developing the protocols also helped to troubleshoot underlying experimental setup issues that created poorer reversibility and reproducibility. Overall, this work provides a detailed resource for iron electrochemistry researchers throughout the community developing technology in industrial metal production, long duration energy storage, and beyond.

Benchmarking Protocols

To ensure similar results across multiple labs using a variety of different equipment when studying iron electrochemistry, we develop standard protocols for electrolyte preparation and a baseline electrochemical analysis for both the Fe^{2+} to Fe^0 metal oxidation/reduction reaction and the Fe^{2+} to Fe^{3+} oxidation/reduction reactions. The experiments defined below use commonly available reagents and should not take more than one day to complete. We chose $FeSO_4$ because it is a commonly used iron reagent, and it is inexpensive and non-toxic. The concentration we chose does not necessitate the use of a supporting electrolyte, which may introduce additional complexity as has been observed in multi-cation systems.[35] At pH 2, the Fe^{2+} to Fe^0 and the Fe^{2+} to Fe^{3+} reactions occur at potentials that are insensitive to small changes in pH, and they do not form less soluble iron hydroxide species. For all experiments, iR drop compensation must be performed to accurately deconvolute ohmic, kinetic, and transport overpotentials. There are many methods of iR compensation (e.g., static, current interrupt, etc…), and resistances that derive from extrinsic factors (e.g., cell geometry, electrode surface layers, bubble formation, etc…) may be

mischaracterized as solution iR drop. It is difficult to rigorously control for all of these factors across institutions, and for this reason we recommend a static iR compensation method (90% of full compensation). In our experience, this yields a stable and reproducible electrochemical response that is sensitive to many of the extrinsic factors above and will more clearly indicate issues with the experimental setup. In addition to the detailed descriptions below, we also include a short experimental checklist in the Supporting Information summarizing typical steps for completing these benchmarking experiments.

We define two electrochemical protocols to serve as experimental benchmarks, whose details are summarized in Table 1. The Ferro/Ferri (FF) Protocol entails a potentiostatic scan between 0.2 and 1.3 V vs. SHE at scan rates varying from 10-200 $mV \cdot s^{-1}$. The Fe^{2+} to Fe^{3+} oxidation reaction is well characterized and there are many examples of voltammetry, kinetic, and transport analysis in the literature.[36-39] The Fe^{2+} to Fe^{3+} oxidation reaction happens at 0.77 V vs. SHE, and the results should typically be quasi- or completely reversible for low scan rates and uniform current distributions.[40]

The Ferro/Metal (FM) Deposition Protocol concerns the main reaction of interest for iron metal production: Fe^{2+} to Fe^{0}. We opt to specify peak current densities rather than potential scan windows – the experimenter will more effectively be able to diagnose a problem (i.e. a faulty reference electrode) if the experimenter learns the potential at which the reaction actually occurs rather than seeing the absence of current at a pre-defined potential window. This is a particularly important consideration when moving beyond this standardization protocol, as changes in electrolyte/ligand chemistry can induce significant shifts in the iron reduction potential that may be misinterpreted as poor performance if a fixed potential window is always used. As the specific capacitance is an inherent property of the electrode, it can be used as a means of assessing how much the surface of the electrode changes between scans, and to understand if the iron is mostly or only partially removed during oxidation. Capacitive sweeps should be performed between iron deposition scans and compared to tabulated values of GC specific capacitance.[41] The capacitive scans can be validated to make sure that the specific capacitance values obtained are of the correct order of magnitude.

Table 1. Benchmarking procedure details.

Electrolyte	0.1 M $FeSO_4$ adjusted to pH 2 with H_2SO_4.
Working Electrode	Glassy Carbon
Counter Electrode	Iron
Ferro/Ferri (FF) Oxidation and Reduction Protocol	• Perform FM Deposition Protocol before FF Protocol. • Change electrodes between Protocols. • Scan between 0.2 V vs. SHE and 1.3 V vs. SHE at 200, 150, 100, 50, 25, 10 mV $\cdot s^{-1}$. Agitate solution between scans. Use first scan.
Ferro/Metal (FM) Iron Deposition and Stripping	• Scan from 0.2 V vs. SHE to potentials that yield 1, 10, and 25 mA$\cdot cm^{-2}$ current densities. Find closest match to current densities by trial and error. • Perform capacitive scans between iron deposition scans. Monitor change in specific capacitance as indicator of surface quality.

Setting tolerances depends on the goals of the research and the resources available to pursue them, and our goal is to establish a set of baselines and recommendations for reproducible iron electrochemistry; our methodology can be applied more broadly to any other reaction where it is difficult to get consistent results. In addition to standardizing protocols, we developed an easy and affordable experiment which yielded consistent results to test a participating group's experimental apparatus. The purpose of this study is to test the effectiveness of the standardized protocols. In comparing the results, they serve as a troubleshooting tool to understand the circumstances that could adversely impact results and cause confusion between collaborators.

Table 2 discusses remedies to common solution/cell preparation and data gathering pitfalls, and the specific experimental considerations that were standardized are discussed in detail below:

Table 2. Summary of standardized solution and cell preparation procedures.

	PITFALL	REMEDY
General/Solution Prep	Electrochemical experiments are sensitive to impurities.	• 99% min salt purity. Avoid Pb, Mn, Cu impurities. • For chemistry change or iron residue accumulation, clean cell with strong acid, rinse and boil 3-5x in ultrapure water. • Prior to each experiment, rinse, boil, rinse in ultrapure water. • Use ultrapure water to make electrolyte.
	Fe^{2+} spontaneously oxidizes to Fe^{3+}.	• Check salt for signs of oxidation. Pretreat solution to reduce Fe^{3+} if necessary. Store salts in inert atmosphere. • In a sufficiently pure solution, ratio of steady-state oxidation and reduction current should be at least 1000:1. • Fresh solution every day. • Inert gas purge for 40 min 1: Water prior to solution prep. 2: Electrolyte solution prior to and during experiment.

		• pH adjust concentrated solutions prior to salt addition.
	Solution resistance (IR)	• Perform current interrupt (CI) method, use static compensation at 90% of measured value.
	Spontaneous degradation of working/counter electrode in solution.	• Hold WE at fixed potential (0.0 V vs. SHE) during immersion in electrolyte.
Working Electrode (WE)	Resistive layer on glassy carbon electrodes. †	• Cycle in 2M H_2SO_4 for 20 cycles between 0.2 and 2.2 V vs SHE at 100 $mV \cdot s^{-1}$. Referred to below as electrode "polish cycle."
	Bubbles	• Use glassy carbon as the electrode – the bare surface is not a surface favorable to hydrogen production. Otherwise, bubbles are unavoidable. Remove bubbles prior to each scan.
Counter Electrode (CE)	Plating of ions changes concentration.	• Iron CE (≥99.9%) purity.
	Iron CE may produce Fe^{3+} during cycling.	• Separate WE and CE with porous glass frit.
Reference Electrode (RE)	Reference electrode may contaminate experiment.	• Separate WE and RE with salt bridge or use leakless RE.
	Collaborators use different reference electrodes.	• Re-reference potentials to SHE when reporting.
	Reference electrode drifts/ages.	• Verify RE potential against SHE periodically. Buy fresh RE.

†Discovered only after several failed experiment attempts.

Electrolyte Preparation

Knowing the concentration and purity of the salts and solvent are critical to studying electrochemical phenomena. In C-STEEL we are primarily concerned with the Fe^{2+} to Fe^0 reaction, and therefore we focus our protocol development on electrolytes utilizing Fe^{2+} salts, rather than Fe^{3+}. Fe^{2+} spontaneously oxidizes to Fe^{3+} in the presence of oxygen, even in salts from high quality suppliers. Some batches of salt from the same supplier can contain more Fe^{3+} than others. Fe^{3+} will also form in solutions as they age and contact air. For this reason, an inert gas must be sparged into the water prior to electrolyte preparation and into the electrolyte during the experiment. To ensure that the concentration of Fe^{2+} is well known, we recommend using a fresh solution every day, although solutions with well-controlled atmosphere may last multiple days. Because of the

tendency of Fe^{2+} to precipitate spontaneously in solutions of pH > 2, concentrated solutions should be pH adjusted before the Fe salt is added. Although other assays exist involving chelating agents and UV-vis,[42,43] to determine Fe^{3+} contamination, in the spirit of simplicity and accessibility, we opted not to develop this type of protocol in this work.

The wide range of concentrations that groups may be testing also make it important to define tolerances to impurities, as we must know which impurities are the most likely to interfere with the experimental results for a given electrolyte. Researchers investigating high-concentration solutions, who may consume > 1 kg of salt, must also be able to purchase affordable feedstock for their experiments – to do that, they must know which impurities will have a deleterious effect on their results. The main impurities to avoid are lead (Pb), manganese (Mn), and copper (Cu) because of their ubiquity and tendency to react in the standard potential windows where iron will react or co-deposit.[44] In recognition of the significant role impurities can play in defining electrochemical response, we also standardized cell cleaning protocols to set a baseline expectation for cell cleanliness as well as a ceiling for cleanliness – acid cleaning the cell should be done regularly and whenever electrolyte chemistry changes.

Electrode Selection

Because iron reduction (E° = -0.44 V vs. SHE) occurs at a potential that is more negative than hydrogen evolution reaction (HER) (E° = 0.0 V vs. SHE), we selected glassy carbon (GC) working electrodes (WEs); GC is not catalytic for HER, instead inducing a large overpotential that avoids significant HER prior to the initiation of Fe metal deposition. By contrast, metallic substrates can significantly catalyze HER and influence the nucleation and growth of Fe deposits, perturbing or obscuring important features of the Fe electrochemistry we seek to understand. GC has other advantages, in that it minimizes phenomena, such as ion specific adsorption and underpotential deposition, that occur on metallic substrates and may artificially influence the intrinsic iron electrodeposition behavior we seek to study.

Polishing GC surfaces with a 1 μm polish is required to remove any residual metal/impurities present from previous electrochemical experiments. More extensive polishing with finer polishing media is acceptable, but our results suggest this is not necessary. As described below, the mechanical polishing and solvent cleaning regimen does not reliably remove resistive layers on the surface. Several electrochemical protocols have been developed for cleaning of polishing

impurities from glassy carbon electrodes.[45,46] Given the choice of $FeSO_4$ as a benchmarking electrolyte in this work, we adopted a procedure that involves cycling the electrode in 2.0 M H_2SO_4 to avoid any cross-contamination from other anion species (see Experimental Methods and Table *2* for details). To preserve the WE electrode surface quality before the experiment, it should ideally be held at a fixed potential (0.0 V vs. SHE) during immersion to avoid changes in the surface caused by spontaneous adsorption or chemical reaction (e.g., electrode oxidation), which are not well controlled when immersing at open circuit potential (OCP).

Regardless of WE, however, the production of hydrogen bubbles during iron deposition is unavoidable. Depending on the electrode apparatus being used by the lab (rotating cylinder, rotating disc, stagnant disk, etc.) the bubbles may or may not be able to detach from the surface throughout the course of the experiment. It is imperative throughout the course of the work to understand the effect of hydrogen bubbles on data noise, oxidation waves, and change in pH of the electrolyte as the experiment runs. Prior work shows that small bubbles with only one small point of contact on an electrode exert a negligible effect on the available electrochemical area, concentration overpotential, and activation overpotential, even if there are several of them.[47] In this case the main effect from bubbles is an increase in the apparent solution iR drop. If this exerts a large effect on successive scans, it can be mitigated the periodic removal of bubbles from the surface (e.g., via agitation or rotation, if possible), or by modifying the iR compensation settings (if agitation is not possible). If the bubbles accumulate to the point of completely preventing contact between the WE and the electrolyte, the potentiostat feedback system can overcompensate with the CE and ruin the solution and the WE. This can happen if multiple smaller bubbles coalesce to completely block the electrode surface from the solution. For this reason, bubbles should be removed from the electrode by agitation, if at all possible, prior to each experimental run.

In order to avoid unintended reactions at the WE due to crossover, the WE and the counter electrode (CE) must be separated by a barrier such as a porous glass frit. This frit will enable ionic connection but hinder concentration driven ion diffusion between the two electrodes if uncontrolled Fe^{3+} forms spontaneously at the CE when the WE is polarized to reducing potentials. Although it is possible to use materials other than iron as CE when a frit is in place, rates of Fe^{3+} formation will be significant and electrolyte concentration changes may take place, which are difficult to account for and may result in poor reproducibility. For these reasons, the CE should ideally be pure iron (≥99.9%) to attempt to maintain a constant concentration of Fe^{2+} in solution,

as well as minimize the formation of Fe^{3+}. With an iron CE, each ion plated from solution will ideally result in an ion that is donated to the solution by the CE. When using an iron CE, the surface should be cleaned prior to the experiment by abrasion or by dipping in acid to reveal a fresh surface.

Reference electrodes (REs), commonly consisting of Ag/AgCl, generally have porous solution compartments which can emit Ag^+ or Cl^- ions into the solution. To preserve the purity of the electrolyte, we recommend a salt bridge and Luggin capillary to prevent RE ions from contaminating the electrolyte and to enable effective iR drop compensation, respectively. Another possible remedy for this problem is the use of a leakless RE or a sulfate-based RE. We do not standardize the RE used, but we recommend that potentials be re-referenced to the SHE when they are shared to reduce any confusion created by different potential referencing schemes. The RE can become inaccurate as it ages, and so it should be periodically checked against a known potential (e.g. HER).

Results and Discussion

Ferro/Ferri Protocol

The results of the FF Protocol are summarized in Figure 1. Four collaborators from three groups across two separate institutions performed the experiments. Collaborators B and D are from the same group. Tabular data containing the forward sweep peak current densities and their corresponding potentials can be found in Table S1. Due to the hysteretic nature of CV data, the exercise of comparing two voltammograms is not trivial. The data presented represent characteristic CV responses obtained by the individual researchers in their specific electrochemical setups. The results are similar by inspection, and the discrepancies between the results can only be ascertained by examining the numerical data and the numerical analysis in Table 3 and Figure 2. To evaluate the similarity of the data, the following figures of merit were evaluated: peak current density, peak potential, and the separation between the peak potential for the oxidation and reduction reactions, otherwise known as ΔE_p.

For every figure of merit evaluated, there was generally one outlier. The peak potentials for collaborators B-D are very similar and closely grouped, while collaborator A's peak potentials generally lie outside of the 99% confidence interval. Collaborator A's ΔE_p values were also notably higher than collaborators B-D. Regarding the peak current densities, collaborator C's peak current densities were notably higher than collaborators A, B, and D, which is likely correlated with

collaborator C's low (and more reversible) ΔE_p values. The discrepancies between peak current density and ΔE_p tend to increase with higher scan rates.

Collaborators B and D, who were from the same group, had similar peak potential, peak current density, and ΔE_p. This suggests that the use of identical equipment and identical chemicals in an identical location affects the results – hypothetically, if collaborators A and C used the same equipment and chemicals as collaborators B and D, their results would have been within the same range of tolerance. For this reason, the spread of results between collaborators A-D show the hypothetical spread of results if the *same protocol* is followed, whereas the range of results between collaborators B and D show the hypothetical spread of results if the *same materials and same protocol* are used.

To gain further understanding of this reaction, we first use Randles-Ševčík (RS) analysis to evaluate the diffusion coefficients from our CV measurements. Although the RS analysis assumes that the voltammetry is reversible, which, as discussed below, is not necessarily the case for these results, it still provides a reasonable assessment of how comparable the measured CVs are with each other by way of comparing the calculated diffusion coefficients. Any inherent irreversibility manifests in RS analysis as a peak potential dependance on scan rate during voltammetry. The RS equation outlines the dependence of the current density on the square root of the potential scan rate:

$$\boldsymbol{i_p = \left(2.69 \times 10^5\right) n^{\frac{3}{2}} D_r^{\frac{1}{2}} C_r^* \nu^{\frac{1}{2}}} \qquad \text{Equation 2}$$

Where i_p is the peak current density of the scan, n is the number of electrons transferred (n=1), A is the electrode area, D_r is the diffusion coefficient, C_r^* is the concentration of Fe^{2+} in the bulk, and ν is the scan rate. A best-fit line of the peak current density analysis can be used with Equation 2 to calculate a diffusion coefficient, which can be compared between groups and compared to literature values. Figure S1 and **Table 3** shows the RS analysis applied to the entire range of scan rates, which yields diffusivity values that are close to each other and to literature values. Tabulated diffusivity values for Fe^{2+} (7.2×10^{-6} cm^2 s^{-1}) obtained by the Nernst-Einstein relation extrapolated to infinite dilution are higher but within a similar order of magnitude.[48] Other reported diffusivity values for Fe^{2+} obtained by Levich analysis at finite concentrations are lower (6.1×10^{-6} cm^2 s^{-1};[49] 3.9×10^{-6} cm^2 s^{-1};[50] 4.7×10^{-6} cm^2 s^{-1};[51]) and closer to the values we report in this work. However, at higher scan rates there are clear deviations from linearity; for this reason, we chose to employ a

hybrid analysis. Figure 2A and shows the same RS analysis applied to only the low scan rates (10-50 mV·s^{-1}) the results of this fitting which likewise yield diffusivity values that are slightly closer to literature values than those determined from fitting of the full range of scan rates.

Table 3. Ferro/Ferri Protocol - Fe(II) to Fe(III) conversion analysis. Randles-Ševčík model used for low scan rates 10-50 mV·s^{-1} and Nicholson-Shain used for high scan rates 100-200 mV·s^{-1}. The resulting diffusivity values are in good agreement.

Model	Scan Rate	A	B	C	D
	mV·s^{-1}		10^6 cm^2 · s^{-1}		
Randles-Ševčík (all Scan Rates)	10-200	2.04	2.07	3.03	2.53
Randles-Ševčík	10-50	2.75	3.15	3.12	3.89
Nicholson-Shain	100-200	3.03	2.96	3.87	4.57

Above 50 mV s^{-1} there is significant peak potential dependence on scan rate, indicating deviations from ideally reversible behavior. Using tabulated values for the diffusivity and the rate constant we can estimate the Nicholson ψ parameter:[40,52]

$$\psi = \frac{\left(\frac{D_O}{D_R}\right)^{\frac{\alpha}{2}} k^0}{(\pi D_O f v)^{1/2}} \qquad \text{Equation 3}$$

Where D_O is the Fe^{3+} diffusivity, D_R is the Fe^{2+} diffusivity, k^0 is the rate constant, *f* is the Faraday constant divided by the ideal gas constant and the temperature, and *v* is the scan rate. For the purposes of this analysis, we assume α = 0.5. Using the ψ parameter, the FF protocol results should have some quasi-reversible rate dependence. Due to the quasi-reversible nature of the reaction, we can additionally use the method of Nicholson and Shain (NS),[40,53-56] which makes it possible to calculate a diffusion coefficient from a scan-rate dependent reaction displaying irreversible kinetics. The NS method includes the dependence of the electrochemical response on the charge transfer coefficient, α:

$$i_p = -0.4958 \left(\frac{F^3}{RT}\right)^{\frac{1}{2}} \alpha^{\frac{1}{2}} D_r^{\frac{1}{2}} C_r^* v^{\frac{1}{2}} \qquad \text{Equation 3}$$

This hybrid RS and NS analysis (Figure 2), yielded consistent results between institutions, with predicted diffusion coefficients between 2.5 and 5 x 10^{-6} cm^2 s^{-1} for the oxidation wave. Collaborators C and D, who had the lowest ΔE_p values, had higher discrepancies between the predicted diffusivities by the RS and NS methods.

We note that poor current distribution can also create peak potential dependence on the scan rate, and it can be a confounding factor in the accurate quantification of the dependence of peak current on scan rate as it makes a reaction appear more irreversible. Uniformity can be assessed by calculating the Wagner number (Wa) for a disk electrode, assuming Tafel kinetics, via equation 4 below.

$$\boldsymbol{Wa} = \frac{\boldsymbol{4\kappa RT}}{\boldsymbol{\pi F \alpha i_{avg} r}} \quad \text{Equation 4}$$

The Wagner number is a dimensionless quantity which relates kinetic losses to ohmic losses where κ is the ionic conductivity of the electrolyte, R is the universal gas constant, T is temperature, F is Faraday's constant, α is the charge transfer coefficient for the reaction in question, i_{avg} is the average current density at the working electrode and r is the radius of the working electrode. Generally, a Wagner number larger than 5 indicates a uniform current distribution.[57] It is important to note that the Wagner number is a function of the electrode radius and a given electrolyte may exhibit uniform current distribution for one group but not another if using different sized electrodes. Peak current density increases at higher sweep rates which results in a lower Wagner number and less uniform current distribution. This is a possible explanation for the observed irreversibility at higher sweep rates across all groups. In general, the observed deviations from ideally reversible behavior for the $Fe^{2+/3+}$ couple are surprising and their origin is unclear at this time. Additional investigation into the precise mechanisms resulting in the non-ideally reversible behavior of this nominally outer-sphere reaction are outside the scope of this study but are of significant fundamental interest.

Overall, the FF protocol, combined with the RS and NS analysis, made it possible to validate the electrolyte preparation and experimental apparatus – it proved to be the most useful exercise of this benchmarking effort, as it informed us that we needed to take extra measures to clean the surface of our electrode prior to each experiment. This protocol is also useful to check if an electrode surface is fouled, as this will influence the apparent reversibility of the couple even if iR drop is fully compensated. Since the iron systems are reasonably well understood, we can also determine if current distribution is uniform for a given electrode. Given the qualitative and quantitative similarities between the RS analysis, NS analysis, and the other figures of merit for the FF protocol, we can assert with a high degree of confidence that we are evaluating the same process and can make direct, apples-to-apples comparisons between our results. To return to our

question: are we measuring the same chemistry? The results of the FF protocol indicate that the answer is yes.

Ferro/Metal Protocol

Results of the FM Protocol are summarized in Figure 3. The CVs are qualitatively similar by inspection. Because the achievement of specific current densities during CV for metal deposition processes is a trial-and-error process due to the stochastic nature of metal nucleation and growth, the goal was to achieve the 1, 10, and 25 $mA \cdot cm^{-2}$ current densities as closely as possible. Tabular data containing the current maxima and minima with their corresponding potentials can be found in Table S2. The specific capacitance values suggest that the surface remained consistent throughout the duration of the scans for all collaborators (Figure S2). In general, the specific capacitance decreased with successive scans, except for collaborator D who did not see a monotonic decrease in specific capacitance with successive scans. Between collaborators, the measured specific capacitance values are in different orders of magnitude, which emphasizes that even with the same notional electrode preparation that the roughness and other surface characteristics can be notably different.

The reduction sweep minima form distinct clusters because we intentionally set the current density targets far apart. Some of the spread in the current density peaks is due to the trial-and-error nature of hitting a particular current density target by specifying the minimum potential of the sweep. The potential-current density relationship becomes more uniform between collaborators as the current density increases. Subtle differences between the electrode preparation or other experimental conditions are less apparent in the results at higher current densities.

In general, collaborators B-D saw similar oxidation current density peaks and potentials within current densities; collaborator A observed significantly higher oxidation current densities for the 25 $mA \cdot cm^{-2}$ current density. The oxidation peaks are less correlated with the magnitude of the reduction peaks because of parasitic hydrogen evolution and differences in the absolute amount of iron metal plated in each CV. The deposit roughness can also influence the shape of the oxidation wave, which can change with the current distribution and the electrode quality. The confidence ellipses of the oxidation peaks (Figure 4D) overlap with each other, meaning that the different experiments did not produce quantitatively distinct oxidation peaks. To return to our question: are

we measuring the same chemistry? The similarities of the FM protocol suggest that we are measuring the same chemistry.

Protocol Troubleshooting

The effort of trying to conduct the same experiment under the same conditions and comparing results between groups yielded a quick and effective means of troubleshooting experimental problems, which ultimately improved the results of experiments outside of the benchmarking scope. The most notable example: the first iterations of the experiment (before the H_2SO_4 electrochemical post-polishing step was implemented, see Table 2) yielded $Fe^{2+/3+}$ oxidation and reduction waves that were several hundred millivolts apart, indicating an extra resistance layer on the electrode (Figures S3-S4). The CV results of an electrode that has not had the post-polish cycle differ by electrode vendor. This result was corroborated with other work on iron redox flow batteries, which proposes that glassy carbon can require a similar post-polish process by cycling the polished, clean glassy carbon electrode in 2.0 M sulfuric acid solution at 100 $mV \cdot s^{-1}$ between 0 and 2 V for 10 consecutive cycles.[38,46] This is surprising given that the oxidation of Fe^{2+} to Fe^{3+} is canonically an outer-sphere reaction. Other work on vanadium redox flow batteries has confirmed that different surface treatments yield different reaction kinetics.[58] Measurement of the surface chemistry of the electrode after undergoing the post-polish cycle was outside the scope of this work; the post-polish cycle may result in a different surface termination of the electrode or it may simply oxidize off any adsorbed foulants, such as isopropyl alcohol used to clean the electrode surface after mechanical polishing. Regardless of the mechanistic explanation, the post-polish cycle yielded significantly more reversible oxidation and reduction waves closer to their standard potentials as seen in Figure 1.

We determined that we needed to do an electrode post-polish cycle only after we produced data with poor reversibility – we did not know at the beginning that we would need to activate the glassy carbon electrode. The previous work on vanadium flow batteries demonstrates that not all reactions have the same degree of sensitivity to surface chemistry, and that it must be evaluated on a case-by-case basis.[58] This further illustrates the value of this exercise in fine-tuning the experimental setup to the reaction chemistry. Sourcing of the glassy carbon electrode can also influence the formation of an inactive surface resistive layer – electrodes from the same supplier showed similar surface resistive characteristics across institutions. The solution to the problem is

ultimately the same – use an electrode post-polish cycling procedure, but the similarity of the resistive layer based on electrode vendor and ability to reproduce across institutions was surprising and helped us to diagnose issues with the experimental protocol. We also note that during this exercise, comparison of results from the Randles-Ševčík and Nicholson-Shain analysis highlighted differences in the way that some calculations and unit conversions were made, such that they could be quickly reconciled. The result was a high level of confidence in the validity of the results.

The benchmarking exercise also helped to quickly and effectively diagnose problems with experimental setup, such as the physical separator between the working and counter electrode, and an aging reference electrode (Figure S5). The aging reference electrode yielded potentials 0.2 V lower than the results reported in Figure 3, which we were only able to ascertain by comparing to the other collaborators' results. In addition to the reference electrode, the benchmarking exercise elucidated the effect of higher levels of Fe^{3+} impurities in the $FeSO_4$ salt. The systematic deviation seen in the FM protocol results (Figure S6) included lower overpotential deposition onset, and an additional reduction feature that is significantly positive (~0.4 V) of iron metal deposition. These problems can be challenging to diagnose and require the exploration of time-consuming hypotheticals, sometimes wasting weeks or months with detective work. In this case, purchasing a new salt with reduced Fe^{3+} impurities resolved the issue. We note that another possible mitigation strategy for Fe^{3+} impurities is bulk electrolysis, either in an RDE or flow cell setup, to electrochemically reduce Fe^{3+} to Fe^{2+} prior to running the benchmarking protocol. RDE along with Levich analysis can also assist in quantifying Fe^{3+} concentration. Although not an explicit remedy, UV-Vis spectroscopy can also be used to assess whether a significant fraction of Fe^{3+} is present in the electrolyte prior to performing the benchmark tests.[59,60]

Limitations to Protocol Development

Finally, we note some limitations and opportunities for further development of these benchmarking protocols and standardized experimental results. The scope of our testing – 4 researchers over 3 independent laboratories and 2 institutions – is helpful for evaluating the extent to which these protocols are reproducible against variability in setup, materials and other topics. This said, even broader testing across a greater variation of electrochemical setups and materials suppliers would improve the statistical certainty with which we can confidently assert that the results here are representative of the "true" electrochemical response of aqueous $FeSO_4$

electrolytes. Features such as the surprising sensitivity of the nominally outer sphere $Fe^{2+/3+}$ redox discussed above highlight that there is still much to be learned, even for this nominally "simple" system. Furthermore, although our protocol specifies a number of standardized parameters and expectations, we have not performed a systematic analysis of the relative impact of each parameter on the resulting voltammetry. This would be valuable to understand if a given group is unable to meet some of the specified criteria, so that the impact on reproducibility can be better quantified. Ultimately, the standard we strive for is greater transparency – a more complete description of methods used and limitations to interpretation due to uncontrolled parameters in a given experiment. Developing protocols such as these enable a consistent point of reference against which other work in the field can be contextualized in order to better understand what represents real advances vs inconsistent methodology. We anticipate that adoption of these procedures will serve as an important first step towards developing a more uniform set of baselines to help accelerate the development and deployment of iron-based electrodeposition technologies.

Conclusion

This work provides a helpful guide for how to carry out Fe^{2+} electrochemistry experiments. A scheme for standardizing iron electrochemistry experiments has been described and tested. We consider electrolyte and solution preparation; reference electrode selection; electrode selection and preparation; cell geometry selection; and the experimental protocol necessary to produce reproducible results comparable to other published and tabulated values. Common challenges, such as bubble formation, Fe^{3+} contamination, and electrode resistive layers are also addressed and contextualized.

This methodology has the utility of allowing for quick experimental setup troubleshooting. Its application between different labs and institutions allows for the rapid development of best practices by elucidating tolerances to different incidental experimental conditions that would otherwise be opaque to outside readers. The highest spreads in the data tended to be in the reduction onset and oxidation onset overpotentials, and these are therefore the least universally reproducible. The other clear result is that the surface quality of the electrode has an oversized effect on the reversibility of the reaction, and the presence of Fe^{3+} impurities can create early onset reduction and increase the magnitude of the oxidation wave. This standardization approach has yielded data that show minor variations and the same overall result.

Moving forward, these protocols provide a baseline standard enabling a group to reliably report results and ensure that new phenomena derive from the specific chemistry under investigation and not extrinsic factors relating to the electrochemical cell assembly or other experimental errors. Although we focus on iron, the methodology reported can be extended beyond iron into other electrodeposition systems by developing comparable control over cell setup/cleanliness, electrolyte purity, and electrochemical methodology. We anticipate its utility well beyond work in C-STEEL, and we hope that our methodology and results will aid in the creation of robust datasets for fundamental studies of Fe^{2+} electrochemistry that can enable new, predictive understanding of this technologically important redox couple.

Acknowledgements

This work was supported as part of the Center for Steel Electrification by Electrosynthesis (C-STEEL), an Energy Earthshot Research Center funded by the U.S. Department of Energy, Office of Science, Basic Energy Sciences (BES) and Advanced Scientific Computing Research (ASCR).

References

1 Iron and Steel Technology Roadmap. (IEA, Paris, 2020).

2 Braun, T., Wallace, C., Pham, Q., Nijhawan, S. & Alexander, C. L. Electrochemistry in Action: Iron and Steel Manufacturing. *The Electrochemical Society Interface* **33**, 38 (2024). https://doi.org/10.1149/2.F06242IF

3 Hawthorne, K. L., Petek, T. J., Miller, M. A., Wainright, J. S. & Savinell, R. F. An Investigation into Factors Affecting the Iron Plating Reaction for an All-Iron Flow Battery. *Journal of The Electrochemical Society* **162**, A108 (2015). https://doi.org/10.1149/2.0591501jes

4 Liu, J., Webb, T. M., Ortiz-Castillo, J., Qin, Y. & Gao, T. Thermodynamics of Transition Metal Electrodeposition in Concentrated Aqueous Electrolytes. *The Journal of Physical Chemistry C* **130**, 2091-2106 (2026). https://doi.org/10.1021/acs.jpcc.5c06609

5 Hawthorne, K. L., Wainright, J. S. & Savinell, R. F. Maximizing plating density and efficiency for a negative deposition reaction in a flow battery. *Journal of Power Sources* **269**, 216-224 (2014). https://doi.org/https://doi.org/10.1016/j.jpowsour.2014.06.125

6 Hruska, L. W. & Savinell, R. F. Investigation of Factors Affecting Performance of the Iron-Redox Battery. *Journal of The Electrochemical Society* **128**, 18 (1981). https://doi.org/10.1149/1.2127366

7 Malkhandi, S., Yang, B., Manohar, A. K., Prakash, G. K. S. & Narayanan, S. R. Self-Assembled Monolayers of n-Alkanethiols Suppress Hydrogen Evolution and Increase the Efficiency of Rechargeable Iron Battery Electrodes. *Journal of the American Chemical Society* **135**, 347-353 (2013). https://doi.org/10.1021/ja3095119

8 Manohar, A. K. *et al.* A High Efficiency Iron-Chloride Redox Flow Battery for Large-Scale Energy Storage. *Journal of The Electrochemical Society* **163**, A5118 (2016). https://doi.org/10.1149/2.0161601jes

9 Hawthorne, K. L., Wainright, J. S. & Savinell, R. F. Studies of Iron-Ligand Complexes for an All-Iron Flow Battery Application. *Journal of The Electrochemical Society* **161**, A1662 (2014). https://doi.org/10.1149/2.0761410jes

10 He, Z. *et al.* Iron metal anode for aqueous rechargeable batteries. *Materials Today Advances* **11**, 100156 (2021). https://doi.org/https://doi.org/10.1016/j.mtadv.2021.100156

11 Gimenez-Garcia, I. & Forner-Cuenca, A. Elucidating the influence of electrolyte additives on iron electroplating performance. *Electrochimica Acta* **498**, 144509 (2024). https://doi.org/https://doi.org/10.1016/j.electacta.2024.144509

12 Izaki, M. in *Modern Electroplating* 309-326 (2010).

13 Feng, G. *et al.* Hydrotrope-enabled high concentration aqueous electrolytes for reversible and sustainable iron metal anodes. *Nature Communications* **16**, 11055 (2025). https://doi.org/10.1038/s41467-025-65160-w

14 Jung, M. S. *et al.* Enhanced Reversibility of Iron Metal Anode with a Solid Electrolyte Interphase in Concentrated Chloride Electrolytes. *Advanced Materials* **37**, 2419664 (2025). https://doi.org/https://doi.org/10.1002/adma.202419664

15 Keddam, M., Mottos, O. R. & Takenouti, H. Reaction Model for Iron Dissolution Studied by Electrode Impedance: I . Experimental Results and Reaction Model. *Journal of The Electrochemical Society* **128**, 257 (1981). https://doi.org/10.1149/1.2127401

16 Keddam, M., Mattos, O. R. & Takenouti, H. Reaction Model for Iron Dissolution Studied by Electrode Impedance: II . Determination of the Reaction Model. *Journal of The Electrochemical Society* **128**, 266 (1981). https://doi.org/10.1149/1.2127402

17 Díaz, S. L., Calderón, J. A., Barcia, O. E. & Mattos, O. R. Electrodeposition of iron in sulphate solutions. *Electrochimica Acta* **53**, 7426-7435 (2008). https://doi.org/https://doi.org/10.1016/j.electacta.2008.01.015

18 Smith, G. & Dickinson, E. J. F. Error, reproducibility and uncertainty in experiments for electrochemical energy technologies. *Nature Communications* **13**, 6832 (2022). https://doi.org/10.1038/s41467-022-34594-x

19 Kempler, P. A. & Nielander, A. C. Reliable reporting of Faradaic efficiencies for electrocatalysis research. *Nature Communications* **14**, 1158 (2023). https://doi.org/10.1038/s41467-023-36880-8

20 McCrory, C. C. L., Jung, S., Peters, J. C. & Jaramillo, T. F. Benchmarking Heterogeneous Electrocatalysts for the Oxygen Evolution Reaction. *Journal of the American Chemical Society* **135**, 16977-16987 (2013). https://doi.org/10.1021/ja407115p

21 Ehelebe, K. *et al.* Benchmarking Fuel Cell Electrocatalysts Using Gas Diffusion Electrodes: Inter-lab Comparison and Best Practices. *ACS Energy Letters* **7**, 816-826 (2022). https://doi.org/10.1021/acsenergylett.1c02659

22 Wei, C. *et al.* Recommended Practices and Benchmark Activity for Hydrogen and Oxygen Electrocatalysis in Water Splitting and Fuel Cells. *Advanced Materials* **31**, 1806296 (2019). https://doi.org/https://doi.org/10.1002/adma.201806296

23 Appelhaus, S. *et al.* Benchmarking performance: A round-robin testing for liquid alkaline electrolysis. *International Journal of Hydrogen Energy* **95**, 1004-1010 (2024). https://doi.org/https://doi.org/10.1016/j.ijhydene.2024.11.288

24 Bender, G. *et al.* Initial approaches in benchmarking and round robin testing for proton exchange membrane water electrolyzers. *International Journal of Hydrogen Energy* **44**, 9174-9187 (2019). https://doi.org/https://doi.org/10.1016/j.ijhydene.2019.02.074

25 Randau, S. *et al.* Benchmarking the performance of all-solid-state lithium batteries. *Nature Energy* **5**, 259-270 (2020). https://doi.org/10.1038/s41560-020-0565-1

26 Sun, Y.-K. An Experimental Checklist for Reporting Battery Performances. *ACS Energy Letters* **6**, 2187-2189 (2021). https://doi.org/10.1021/acsenergylett.1c00870

27 Stephan, A. K. Standardized Battery Reporting Guidelines. *Joule* **5**, 1-2 (2021). https://doi.org/10.1016/j.joule.2020.12.026

28 Cui, X. *et al.* Data-driven analysis of battery formation reveals the role of electrode utilization in extending cycle life. *Joule* **8**, 3072-3087 (2024). https://doi.org/10.1016/j.joule.2024.07.024

29 Geslin, A. *et al.* Dynamic cycling enhances battery lifetime. *Nature Energy* **10**, 172-180 (2025). https://doi.org/10.1038/s41560-024-01675-8

30 Ward, L. *et al.* Principles of the Battery Data Genome. *Joule* **7**, 238 (2023). https://doi.org/10.1016/j.joule.2022.12.014

31 Preger, Y. *et al.* Degradation of Commercial Lithium-Ion Cells as a Function of Chemistry and Cycling Conditions. *Journal of The Electrochemical Society* **167**, 120532 (2020). https://doi.org/10.1149/1945-7111/abae37

32 Puls, S. *et al.* Benchmarking the reproducibility of all-solid-state battery cell performance. *Nature Energy* **9**, 1310-1320 (2024). https://doi.org/10.1038/s41560-024-01634-3

33 Vargas-Barbosa, N. M. My cell is better than yours. *Nature Nanotechnology* **19**, 419-420 (2024). https://doi.org/10.1038/s41565-024-01607-3

34 Müller, M. *et al.* Guidelines to correctly measure the lithium ion conductivity of oxide ceramic electrolytes based on a harmonized testing procedure. *Journal of Power Sources* **531**, 231323 (2022). https://doi.org/https://doi.org/10.1016/j.jpowsour.2022.231323

35 Bender, J. T. *et al.* Understanding Cation Effects on the Hydrogen Evolution Reaction. *ACS Energy Letters* **8**, 657-665 (2023). https://doi.org/10.1021/acsenergylett.2c02500

36 Gong, K. *et al.* All-Soluble All-Iron Aqueous Redox-Flow Battery. *ACS Energy Letters* **1**, 89-93 (2016). https://doi.org/10.1021/acsenergylett.6b00049

37 Yu, S. *et al.* A low-cost sulfate-based all iron redox flow battery. *Journal of Power Sources* **513**, 230457 (2021). https://doi.org/https://doi.org/10.1016/j.jpowsour.2021.230457

38 Nambafu, G. S. *et al.* Strategically Modified Ligand Incorporating Mixed Phosphonate and Carboxylate Groups to Enhance Performance in All-Iron Redox Flow Batteries. *Advanced Energy Materials* **15**, 2403149 (2025). https://doi.org/https://doi.org/10.1002/aenm.202403149

39 Savinell, R. F. & Wainright, J. S. Iron Flow Batteries. United States patent (2017).

40 Bard, A. J. & Faulkner, L. R. *Electrochemical Methods: Fundamentals and Applications*. (Wiley, 2001).

41 Belazougui, Y. *et al.* Exploring Impact of Various Operating Parameters on the Specific Capacitance at the Glassy Carbon/H2SO4 Interface: A Comparative Analysis Using Electrochemical Characterization. *ChemistrySelect* **9**, e202400750 (2024). https://doi.org/https://doi.org/10.1002/slct.202400750

42 Stookey, L. L. Ferrozine---a new spectrophotometric reagent for iron. *Analytical Chemistry* **42**, 779-781 (1970). https://doi.org/10.1021/ac60289a016

43 Pyenson, H. & Tracy, P. H. A 1,10—Phenanthroline Method for the Determination of Iron in Powdered Milk. *Journal of Dairy Science* **28**, 401-412 (1945). https://doi.org/https://doi.org/10.3168/jds.S0022-0302(45)95191-5

44 Rumble, J. *CRC handbook of chemistry and physics*. Vol. 102 (CRC press Boca Raton, FL, 2017).

45 Kiema, G. K., Aktay, M. & McDermott, M. T. Preparation of reproducible glassy carbon electrodes by removal of polishing impurities. *Journal of Electroanalytical Chemistry* **540**, 7-15 (2003). https://doi.org/https://doi.org/10.1016/S0022-0728(02)01264-0

46 Noack, J. *et al.* The influence of electrochemical treatment on electrode reactions for vanadium redox-flow batteries. *Journal of Energy Chemistry* **27**, 1341-1352 (2018). https://doi.org/https://doi.org/10.1016/j.jechem.2018.03.021

47 Logar, A. *et al.* Bubble Trouble: Quantifying the Effects of Bubbles on the Electrochemical Interface. *ACS Catalysis* **15**, 6380-6385 (2025). https://doi.org/10.1021/acscatal.5c00144

48 John Newman, K. E. T.-A. *Electrochemical Systems*. 3rd edn, 284 (John Wiley & Sons, Inc., 2004).

49 Angell, D. & Dickinson, T. The kinetics of the ferrous/ferric and ferro/ferricyanide reactions at platinum and gold electrodes: Part I. Kinetics at bare-metal surfaces. *Journal of Electroanalytical Chemistry and Interfacial Electrochemistry* **35**, 55-72 (1972).

50 Morrison, B., Striebel, K., Ross Jr, P. & Andricacos, P. Kinetic studies using a rotating cylinder electrode: Part I. Electron transfer rates in ferrous/ferric sulfate on platinum. *Journal of electroanalytical chemistry and interfacial electrochemistry* **215**, 151-160 (1986).

51 Ye, J. H. & Fedkiw, P. S. Effects of Toluene and Benzoic Acid on the Kinetics of Ferrous Oxidation on Pt and Nafion-Coated Pt Electrodes. *Journal of the Electrochemical Society* **141**, 1483 (1994).

52 Nicholson, R. S. Theory and Application of Cyclic Voltammetry for Measurement of Electrode Reaction Kinetics. *Analytical Chemistry* **37**, 1351-1355 (1965). https://doi.org/10.1021/ac60230a016

53 Shen, D., Steinberg, K. & Akolkar, R. Avoiding Pitfalls in the Determination of Reliable Electrochemical Kinetics Parameters for the Cu2+ → Cu1+ Reduction Reaction in Deep Eutectic Solvents. *Journal of The Electrochemical Society* **165**, E808 (2018). https://doi.org/10.1149/2.1011814jes

54 Randles, J. E. B. A cathode ray polarograph. Part II.—The current-voltage curves. *Transactions of the Faraday Society* **44**, 327-338 (1948). https://doi.org/10.1039/TF9484400327

55 Ševčík, A. Oscillographic polarography with periodical triangular voltage. *Collection of Czechoslovak Chemical Communications* **13**, 349-377 (1948).

56 Nicholson, R. S. & Shain, I. Theory of Stationary Electrode Polarography. Single Scan and Cyclic Methods Applied to Reversible, Irreversible, and Kinetic Systems. *Analytical Chemistry* **36**, 706-723 (1964). https://doi.org/10.1021/ac60210a007

57 Jeganathan, V. S., Sinclair, N. & Akolkar, R. Kinetics Measurements in Resistive Electrolytes Using Ring-Disk Electrode: Ring as Current "Shield" Enables Uniform Disk

Current Distribution. *ACS Electrochemistry* **1**, 1101-1109 (2025). https://doi.org/10.1021/acselectrochem.4c00238

58 Bourke, A. *et al.* Electrode Kinetics in All-Vanadium Flow Batteries: Effects of Electrochemical Treatment. *ECS Transactions* **66**, 181 (2015). https://doi.org/10.1149/06608.0181ecst

59 Fu, Z. & Chen, R. Study of Complexes of Tannic Acid with Fe(III) and Fe(II). *Journal of Analytical Methods in Chemistry* **2019**, 3894571 (2019). https://doi.org/https://doi.org/10.1155/2019/3894571

60 Korolev, V. V. & Bazhin, N. M. The absorption spectra of aqueous solutions of ferrous ions in the UV region. *Journal of Applied Spectroscopy* **20**, 626-629 (1974). https://doi.org/10.1007/BF00607460

61 Matplotlib Development, T. *Plot a confidence ellipse of a two-dimensional dataset*, <https://matplotlib.org/devdocs/gallery/statistics/confidence_ellipse.html> (2025).

Figures

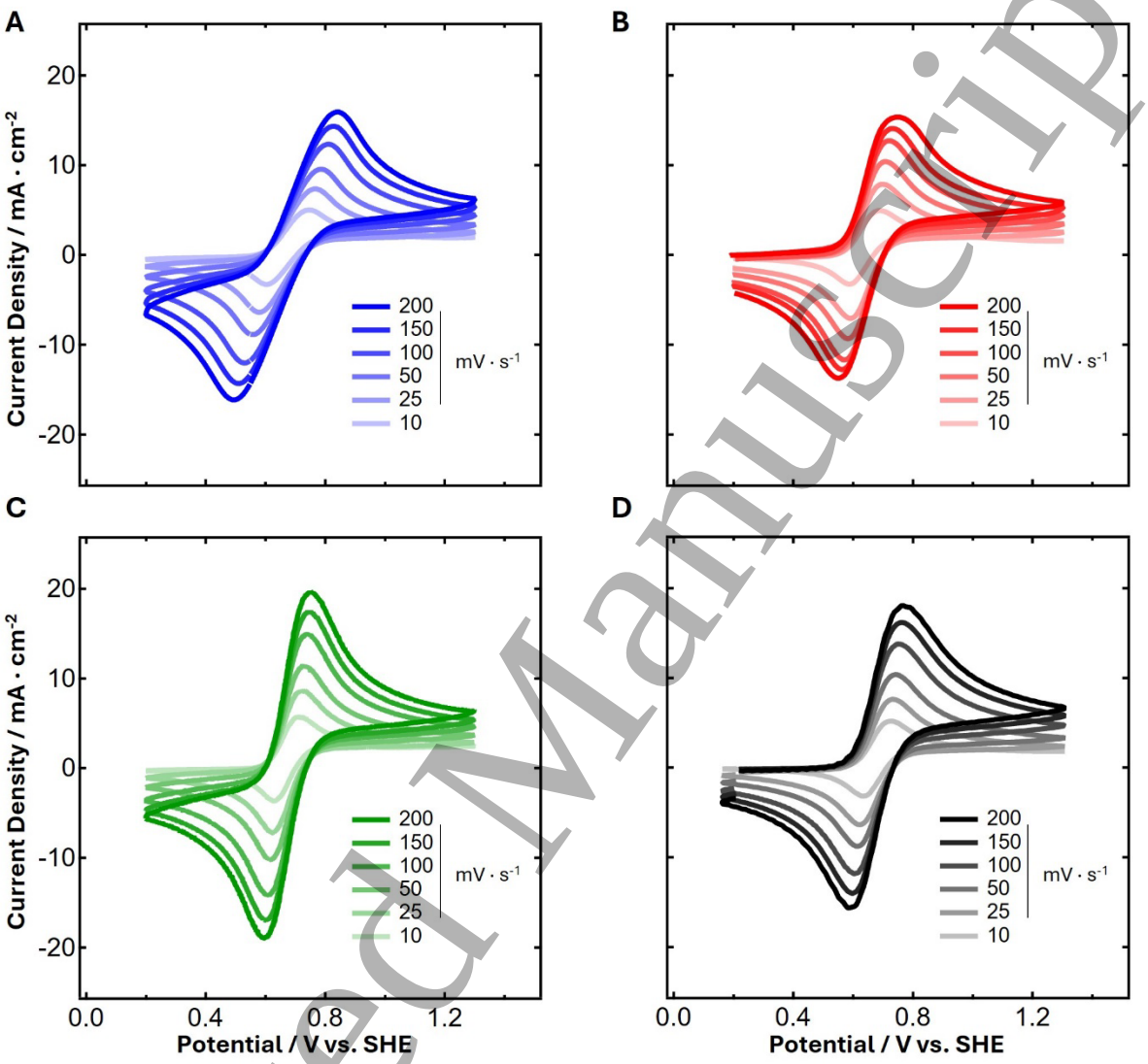

Figure 1. Ferro/Ferri Protocol – Fe^{2+} to Fe^{3+} conversion results from groups A-D. CVs start at 0.2 V vs. SHE, scan positive to 1.3 V vs. SHE, and return 0.2 V vs. SHE. Electrolyte composition: 0.1 M $FeSO_4$ adjusted to pH 2 with H_2SO_4.

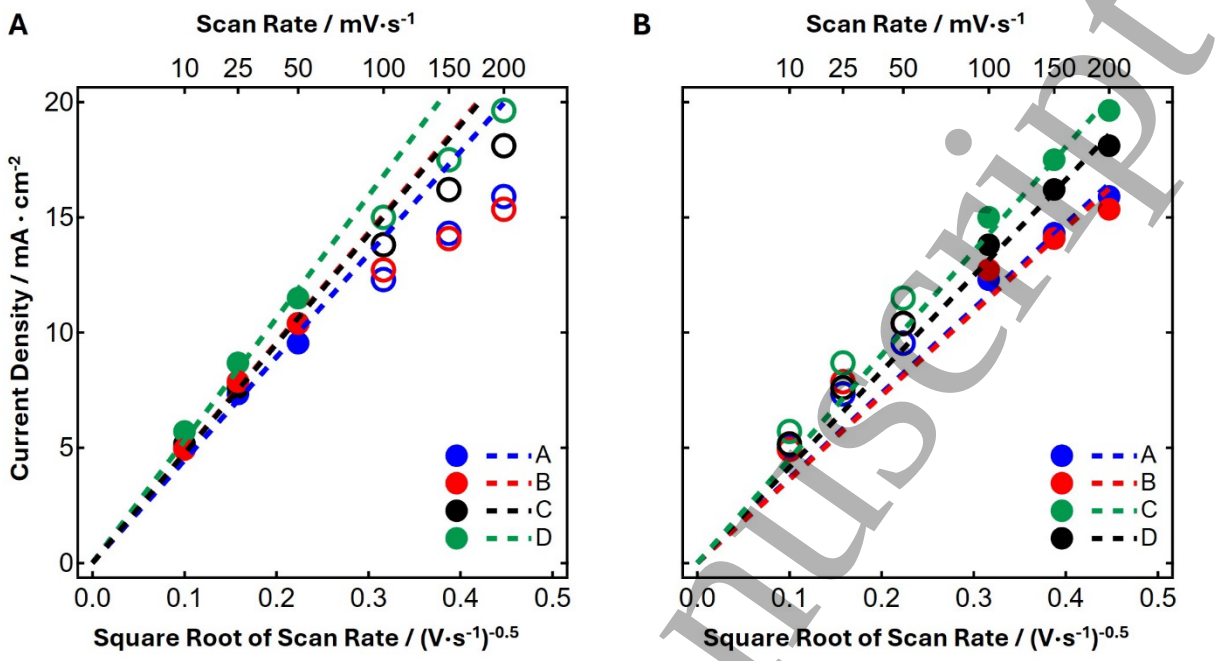

Figure 2. A) Randles-Ševčík Analysis of FF Protocol. Fitting is constrained to scan rates of 10, 25, 50 mV·s^{-1}. B) Nicholson-Shain Analysis of FF Protocol. Fitting is constrained to scan rates of 100, 150, 200 mV·s^{-1}.

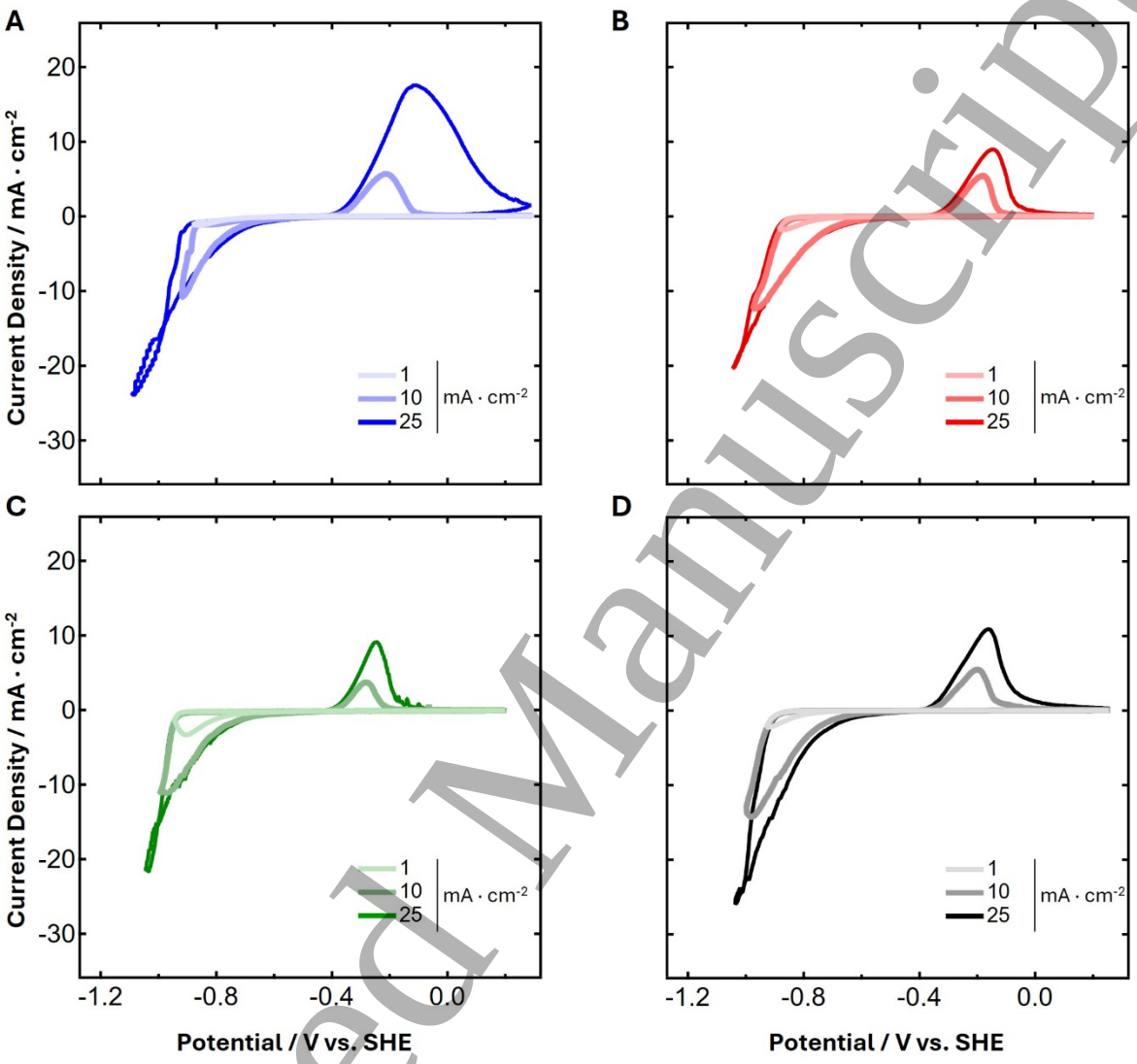

Figure 3. Ferro-Metal Protocol - iron deposition and stripping results from groups A-D. Electrolyte composition: 0.1 M $FeSO_4$ adjusted to pH 2 with H_2SO_4.

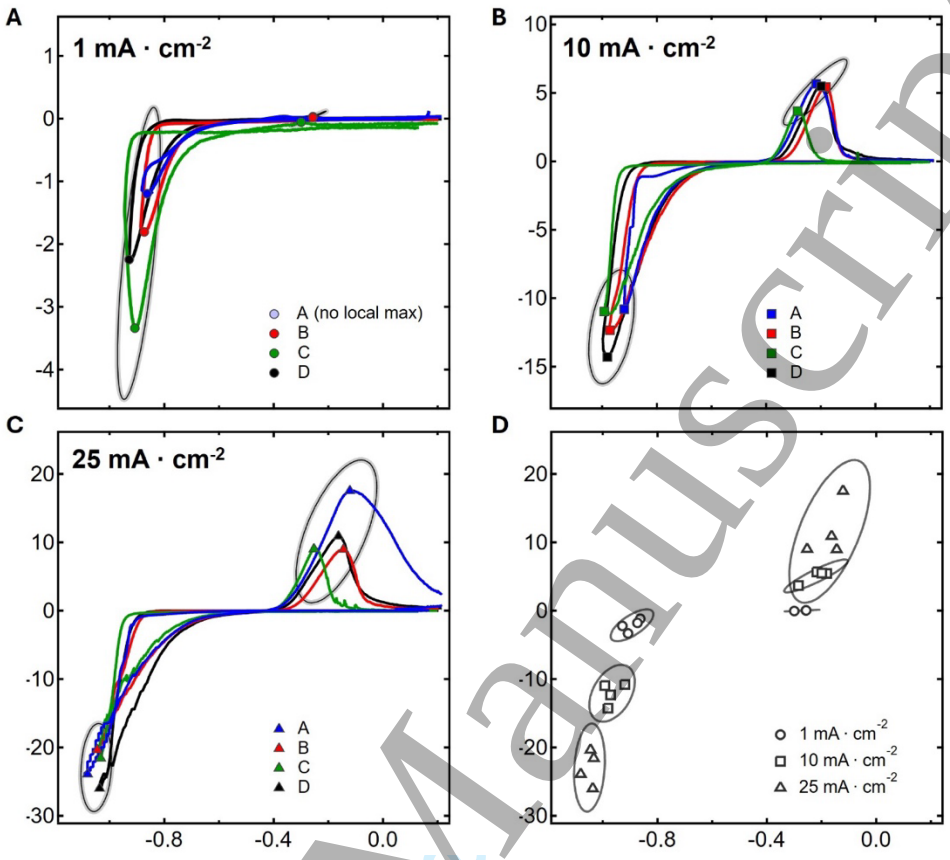

Figure 4. Superposition of deposition curves from Figure 3 with explicit current density maxima and minima. A 99% confidence ellipse has been drawn around the points to demonstrate how tightly correlated the results are. These ellipses assume a standard normal distribution and were calculated using eigenvalues of the Pearson's correlation to set the radii.[61]